Received: 10 April 2023 | Revised: 22 June 2023 | Accepted: 26 June 2023

IET Microwaves, Antennas & Propagation

DOI: 10.1049/mia2.12388

ORIGINAL RESEARCH

Novel antenna array configuration using miniature double box branch-line couplers for wideband circularly polarised applications

Bal S. Virdee[1] | **Tohid Aribi**[2,3] | **Tohid Sedghi**[4,5]

[1]Center for Communications Technology London, Metropolitan University, London, UK

[2]Department of Electrical Engineering, Miandoab Branch, Islamic Azad University, Miandoab, Iran

[3]Artificial Intelligence & Big Data Automation Research Center, Urmia Branch, Islamic Azad University, Urmia, Iran

[4]Department of Electrical Engineering, Urmia Branch, Islamic Azad University, Urmia, Iran

[5]Microwave and Antenna Research Center, Urmia Branch, Islamic Azad University, Urmia, Iran

Correspondence

Bal S. Virdee.
Email: b.virdee@londonmet.ac.uk

Funding information

London Metropolitan University

Abstract

This article presents a wideband circularly polarised (CP) antenna array using a miniaturised double box branch-line coupler. This was achieved by creating a slow wave structure by introducing open-circuit stubs on the inside arms of the branch-line coupler. The 2 × 2 antenna array is made of four CP slot radiating elements excited through 1 × 4 feeding network. Moreover, sequentially rotation method is used to increase the axial-ratio (AR) bandwidth of the array. The CP slot radiating element is fed by coplanar waveguide. The feedline of the horn-shaped radiator includes a circular matching stub. Ground connected asymmetric T-shaped stub, a pair of grounded L-shaped square strips, and single strip line are shown to induce CP and enhance the antenna's 3 dB impedance bandwidth and AR performance. The antenna constituting the array has impedance bandwidth of 2.45 GHz from 4.8 to 7.25 GHz that corresponds to a fractional bandwidth of 40%, and its 3 dB AR extends between 4.8 and 6.25 GHz. Compared to a conventional double-box branch-line coupler the size of the proposed coupler is reduced by 35% by increasing the capacitance of the coupler's arms. This also is shown to increase the impedance bandwidth of the coupler. A 2 × 2 array was fabricated, and its performance verified. Measured results confirm the proposed antenna array exhibits CP covering the bands of WiMAX IEEE 802.16, C-band and ITU-R F386.9. The measured 3 dB AR bandwidth of the antenna array extend from 3 to 7.3 GHz and its impedance bandwidth extends from 3.2 to 9.0 GHz. The antenna array radiates with a peak gain of 11.5 dBic.

KEYWORDS

antennas, microstrip antennas, slot antenna arrays

1 | INTRODUCTION

Modern wireless communication, mobile satellite services, radar tracking, and weather radar systems use popular printed microstrip antenna arrays. This is because of the antenna's attributes of small size, ease of realisation and matching with circular polarisation (CP) [1, 2]. CP features at antenna introduces different types of advantages over linear polarisation specification. In particular, the capability to establish a higher resistant to signal degradation with reliable link between stations without the antenna orientation settlement. Among the general methods to feed the CP array antenna, sequentially rotation method (SRM) has been shown in refs. [3–11] to be effective for improving the polarisation purity and symmetrical radiation patterns over the operational frequency range of the array. Different methodologies have been reported in literature of realising broadband CP antennas which include: (1) loading coplanar waveguide (CPW) fed square aperture antenna with U-shape strip [2–5]; (2) applying slots on the grounded strips [3–6]; and (3) etching a modified T-shaped patch inserted diagonally with respect to the slot [7–9].

The cited references above all have deficiencies of inability to control right- and left-hand CP, narrow 3 dB axial-ratio (AR) bandwidth, and relatively low gain. This paper presents the

design of an antenna array that overcomes these disadvantages. The proposed antenna array has a CP over a broadband frequency range suitable for applications including WiMAX IEEE 802.16, C-band and ITU-R F386.9 applications. The proposed array is made of 2 × 2 slot-elements configuration that are fed with SRM network, as shown in Figure 1. The

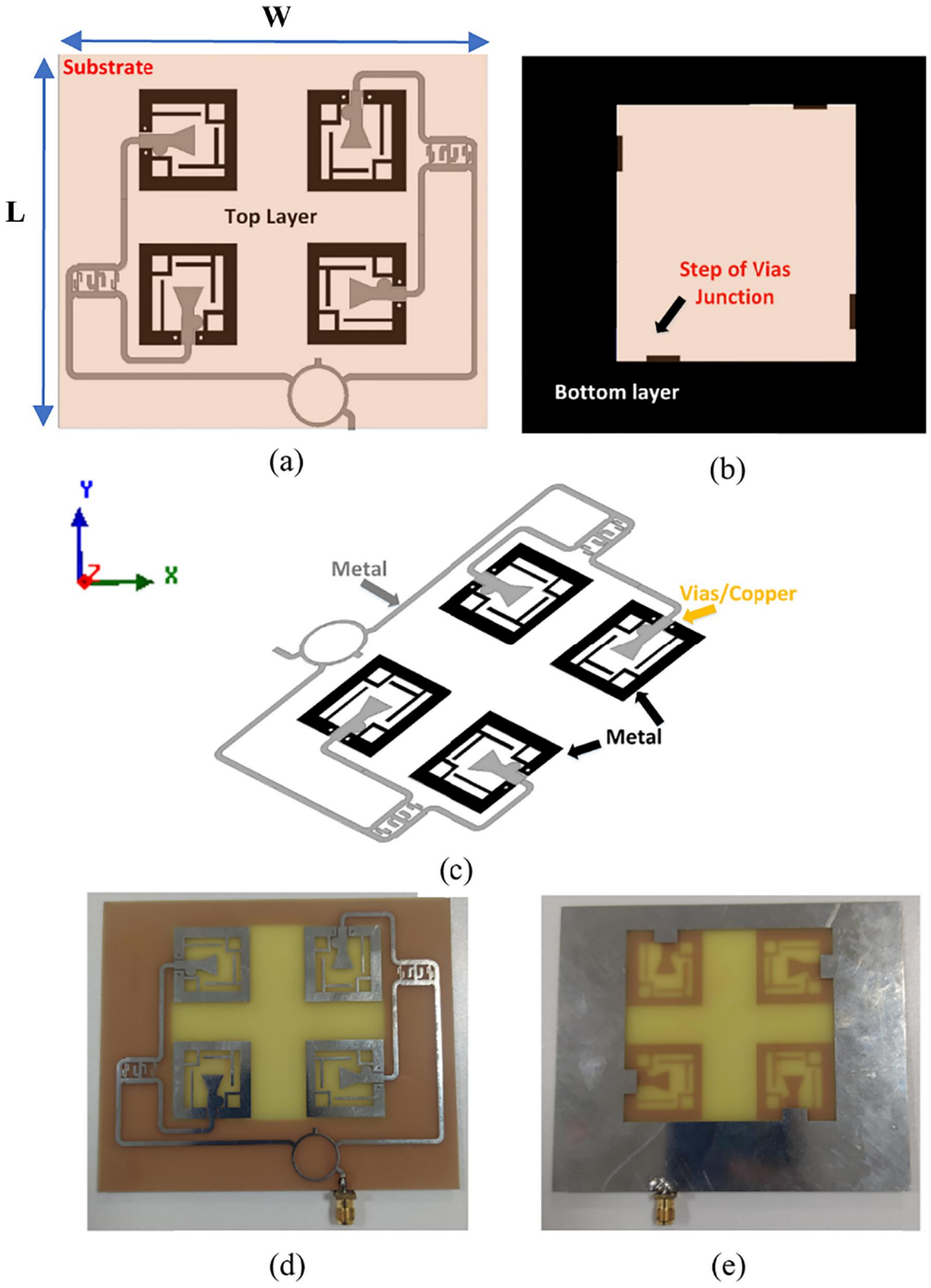

FIGURE 1 Geometry of the proposed array, (a) top-layer, (b) bottom layer, (c) 3D view, (d) top-layer of fabricated antenna, and (e) bottom-layer of fabricated antenna.

elements are designed in specific form and include slots and stubs to realise CP over a broadband. The proposed antenna utilises 4 pairs of vias on the side of each slot-element to increase its inductance to enhance the matching between CPW feed & microstrip-line. Double-box S-shaped coupler is used to improve the array's impedance bandwidth. The distance between the elements in the 2 × 2 planar phased array antenna is 0.65λ (λ is free-space wavelength). The ground-plane under the array has been hollowed to reduce interaction via surface waves, improve the isolation from the feed network and improve the bandwidth [12, 13]. The details of the array's performance are fully analysed and evaluated. The antenna array has a measured peak gain of 11.5 dBic.

2 | ELEMENT DESIGN

The structure of the proposed antenna based on CP slot-element is shown in Figure 2a. The antenna consists of a radiating element that resembles a horn-shaped structure with a semi-circular matching stub at its feedline. Surrounding the radiating element of the antenna is a square shaped ground loop. Connected to the inner space of the ground loop are two open-circuited vertical stubs. A horizontal stub is connected to the open-circuited vertical stub that is in front of the horn-shaped structure. Also, connected at opposite corners inside the ground loop are L-shaped strips. In the proposed structure using a single feedline the electromagnetic interaction between the asymmetric T-shaped stub and the L-shaped strip excite two orthogonal modes (TE_{01} & TM_{11}) with equal amplitudes and CP. Moreover, the structure extends the antenna's AR and impedance bandwidth.

The CP slot-element antenna's performance was optimised utilising Ansys HFSS. The antenna was fabricated on FR4-dielectric substrate with loss tangent of 0.024 and relative permittivity of 4.4. The dimension of the physical parameters of the structure (units in mm) are: $L_1 = 23$, $L_2 = 4$, $L_3 = 9$, $L_4 = 11$, $L_5 = 7.6$, $L_6 = 12.4$, $L_7 = 5.3$, $L_8 = 3.5$, $L_f = 3.1$, $R_f = 1.7$, Gap = 0.3, $L = 90$, and $W = 110$. The overall dimensions of the antenna are 23 × 23 × 0.8 mm^3. Figure 2b,c show the simulated return-loss and AR bandwidth response, respectively, of the single CP slot-element antenna. The antenna has an impedance bandwidth of 2.45 GHz between 4.8 and 7.25 GHz for VSWR <2, and the 3 dB AR bandwidth of 1.45 GHz between 4.8 and 6.25 GHz.

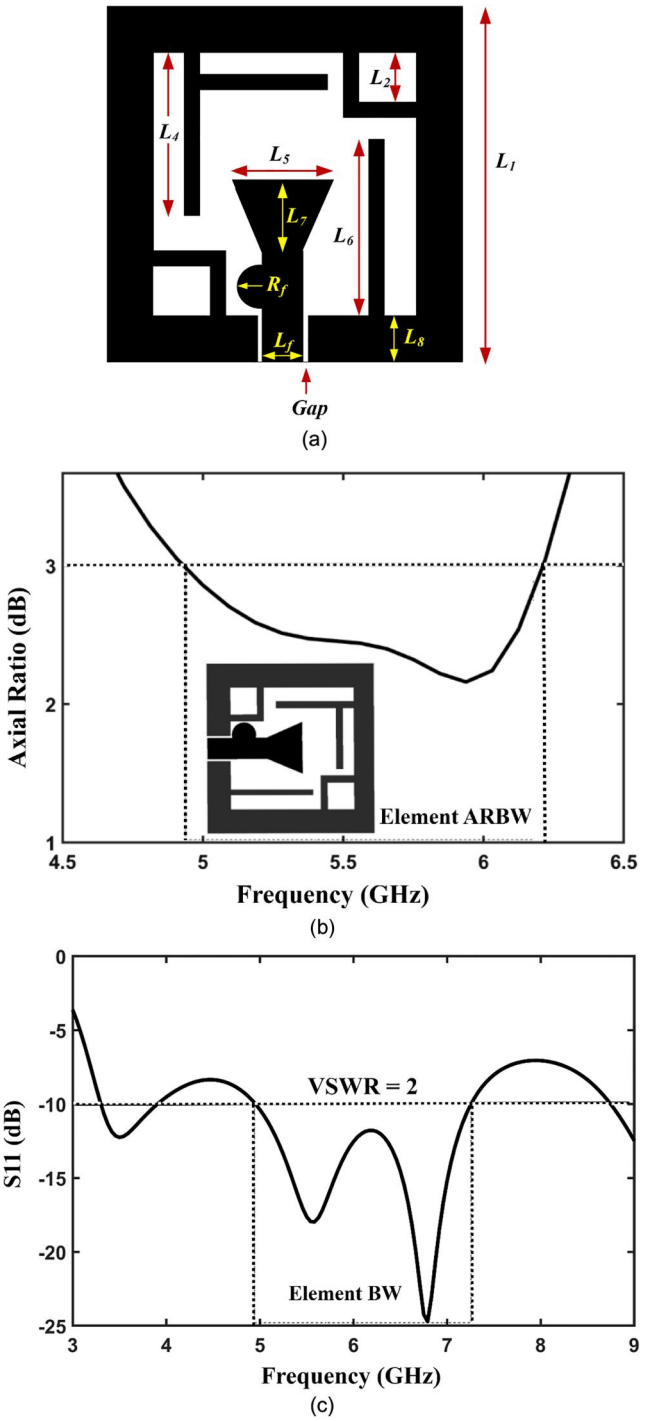

FIGURE 2 (a) Geometry of circularly polarised slot-element configuration, (b) axial-ratio parameter, and (c) return-loss response.

3 | FEED NETWORK DESIGN

The CP slot-element antenna was used to realise a 1 × 4 array. The feed network of the array used here consisted of double box branch-line coupler, shown in Figure 3. The branch-line couplers were cascaded to enhance the coupler's bandwidth. All arms are quarter wavelength in length at the operating centre frequency. The ports are 50 Ω microstrip lines. The double box branch-line coupler's return-loss and differential phase (DP) are shown in Figure 3 respectively. Operational band of is between 4 and 6 GHz, which corresponds to a fractional bandwidth of 40%. Wideband performance and compact coupler size are key features in modern radar and wireless communication systems. A wide operational band is needs in software defined wireless systems to connect with multiple frequency bands and communications standards. The challenge therefore was to reduce the size of the coupler and enhance its operational bandwidth. This was achieved by first

analysing a microstrip transmission line, shown in Figure 4. The transmission line of characteristic impedance, Z_A, and phase velocity, v_p, is given by the following

$$Z_S = \sqrt{L_S/C_S} \tag{1}$$

$$v_P = 1/\sqrt{L_S C_S} \tag{2}$$

where L_S and C_S are the inductance and capacitance per unit length of the line respectively. By adding capacitances in shunt at periodic intervals along the length and making the space

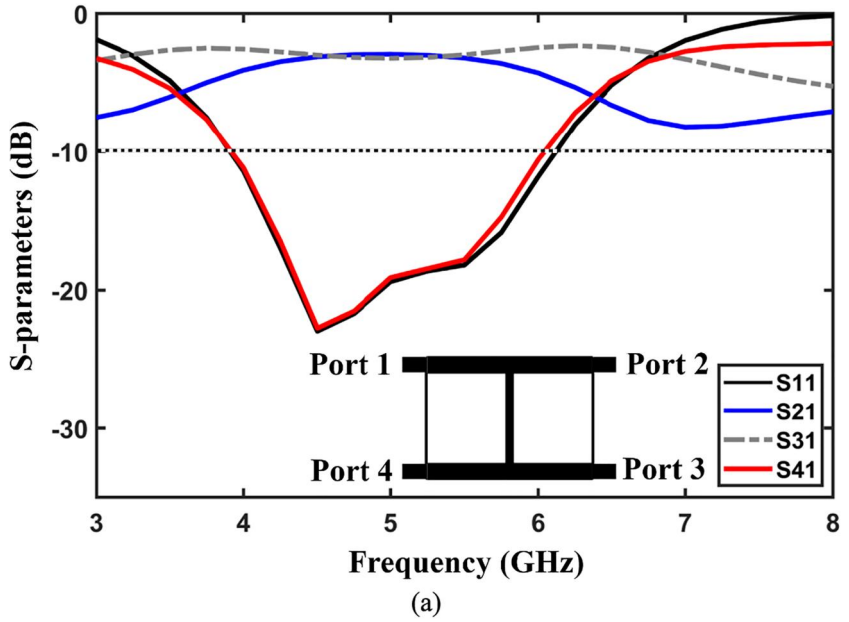

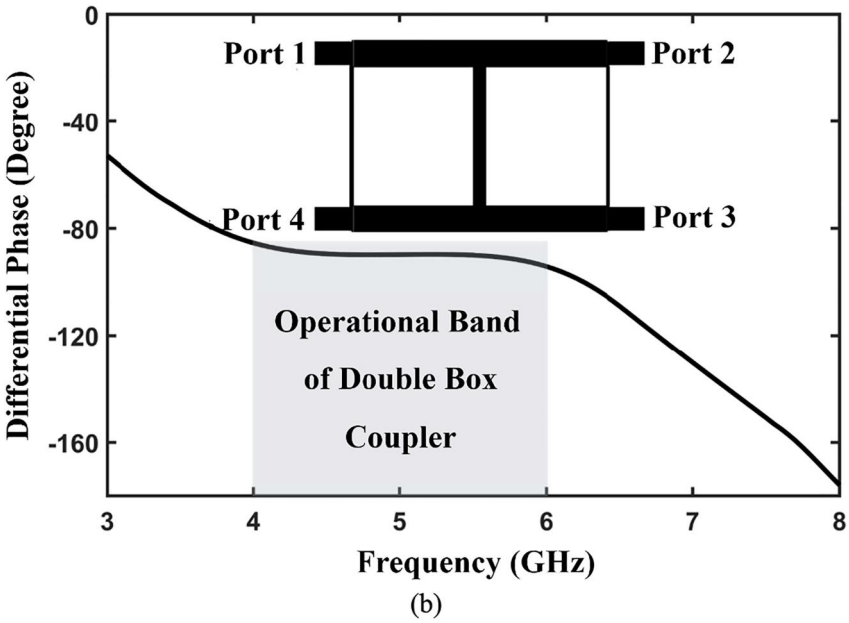

FIGURE 3 (a) Scattering parameters of double box branch coupler, and (b) differential phase response of the double box branch coupler.

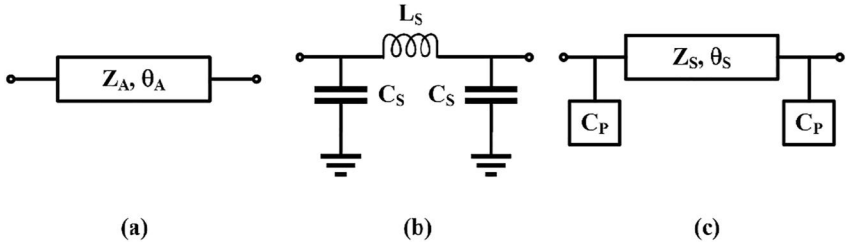

FIGURE 4 Equivalent circuits of a transmission line, (a) conventional microstrip transmission line, (b) equivalent lumped component circuit of a transmission line, and (c) equivalent circuit with distributed components.

between the added capacitors smaller than the operating wavelength, the transmission line can be shown to have an effective characteristic impedance and the phase velocity is given by the following [14]

$$Z_{S,L} = \sqrt{L_S/(C_S + C_P/d)} \tag{3}$$

and

$$v_{P,L} = 1/\sqrt{L_S(C_S + C_P/d)} \tag{4}$$

where C_P is the periodic loaded capacitance at distance d apart over the transmission line. $Z_{S,L}$ and Z_S are the characteristic impedance of loaded and unloaded line respectively. Equations (3) and (4) indicate the effect of loading the transmission line results in the lowering of the effective characteristic impedance and phase velocity. A lowered phase velocity means that an effectively long electric length can be realised with a shorter physical length. If $v_{P,L}$ is the phase velocity of the periodically loaded transmission line, then the electric length θ of this line is given by the following,

$$\theta = l(\omega_o/v_{P,L}) \tag{5}$$

where l is the physical length of the loaded transmission line. The phase velocities of the loaded line and the unloaded line can be related through their respective propagation constants β_o and k_o, as given by the following

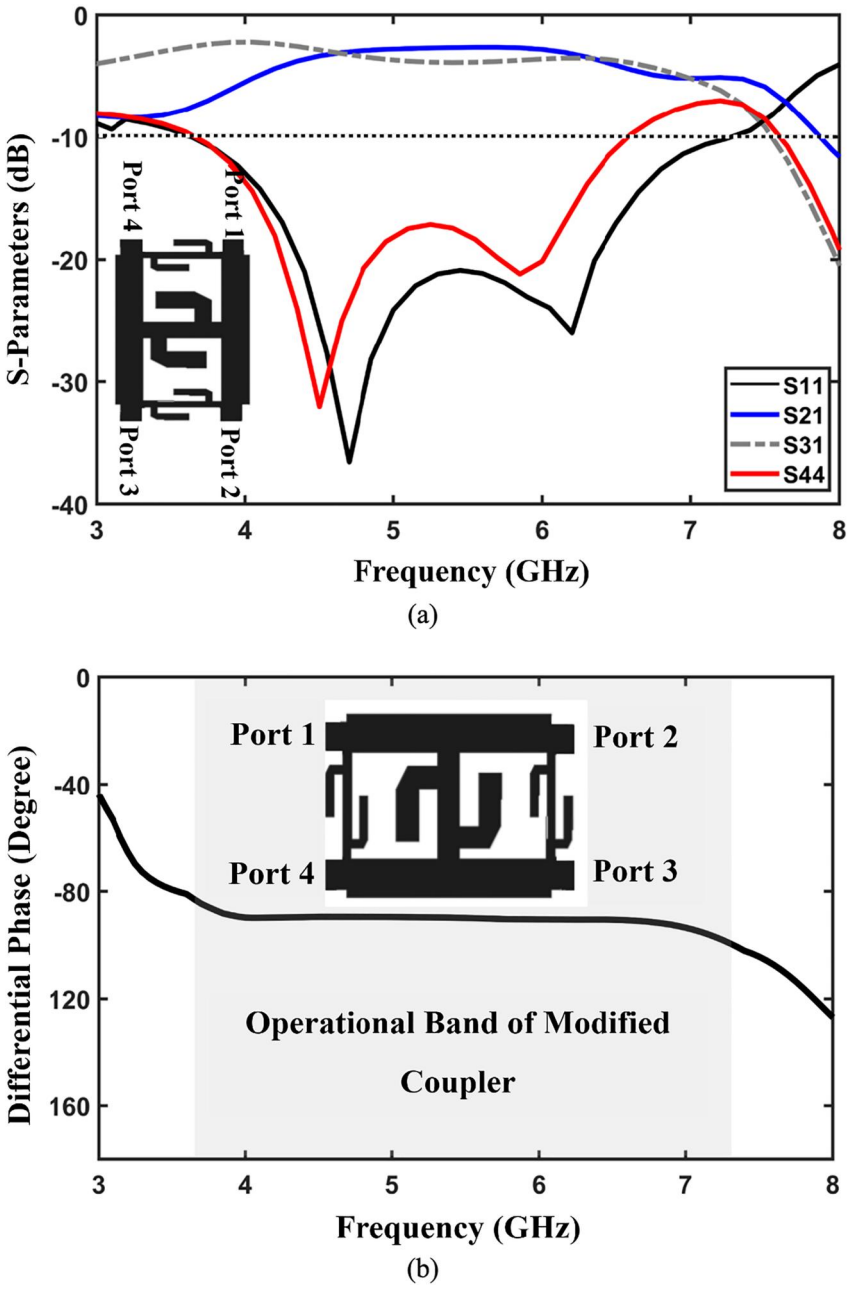

FIGURE 5 (a) Scattering parameters of double box branch coupler with S-shaped stubs and (b) differential phase response of double box branch coupler with S-shaped stubs.

$$v_{P,L} = v_P(k_o/\beta_o) \tag{6}$$

Using Equations (1)–(6), it can be shown that the gap d between the shunt capacitance C_P realised using open circuit stubs are given by

$$d = \theta(Z_{S,L}/Z_S)v_P/\omega_o \tag{7}$$

and

$$C_P = \frac{1}{\omega_o Z_{o,\text{stub}}}\tan\left(\frac{2\pi}{\lambda}l_{\text{stub}}\right) \tag{8}$$

where $Z_{o,\text{stub}}$ and l_{stub} are the characteristic impedance and physical length of the transmission line used as the stub respectively. The open-circuit stubs used to load the inside arms of the coupler where S-shaped, as shown in Figure 5. The distance between the two adjacent elements is 0.65λ. Compared to the conventional double box branch-line coupler the size of the proposed coupler is reduced by 35%.

Figure 5 shows the return-loss and DP of proposed double box branch-line coupler. This coupler has a bandwidth of 3.6 GHz from 3.6 to 7.2 GHz with a corresponding fractional bandwidth of 67%. Compared to the conventional double box branch-line coupler this constitutes a fractional bandwidth increase of 27%.

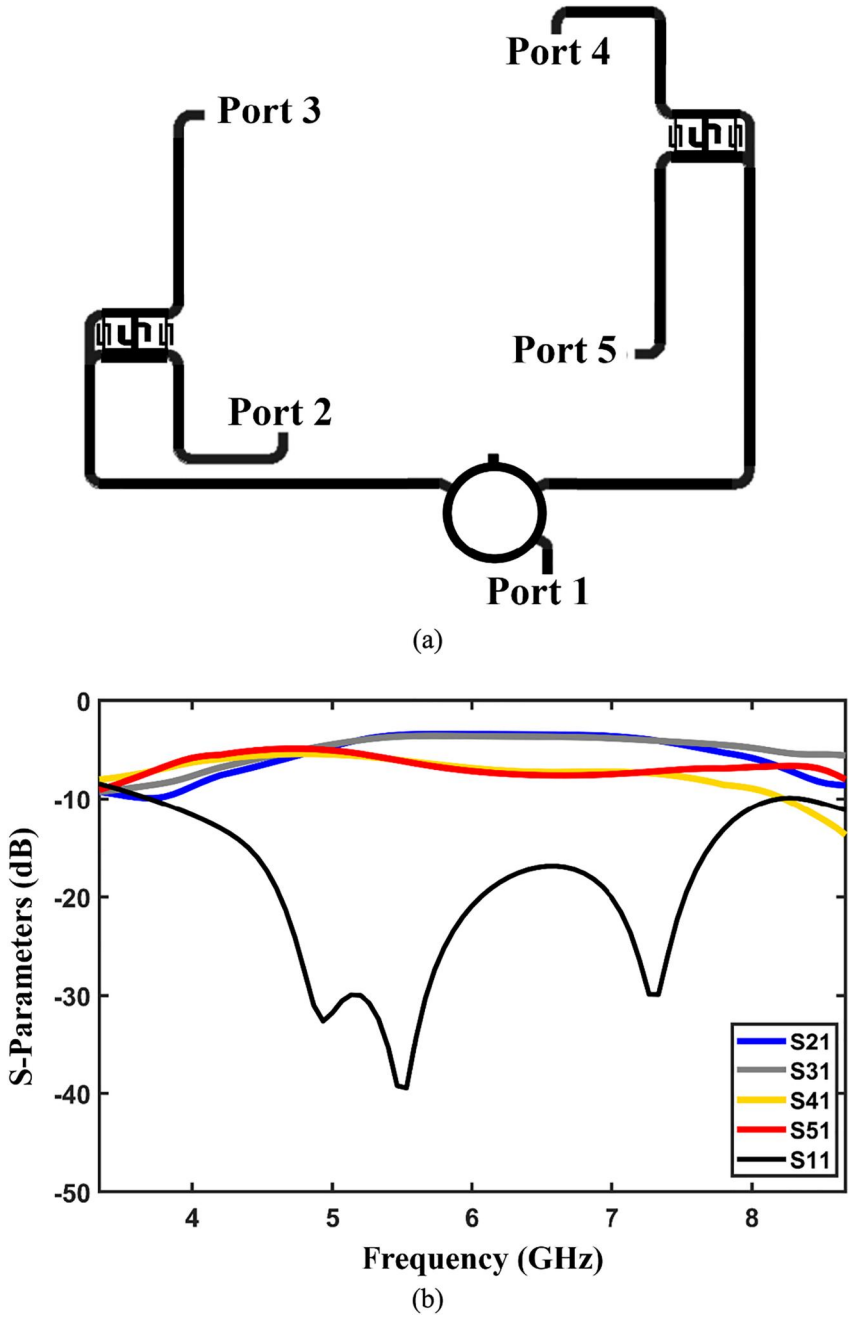

FIGURE 6 (a) Geometry of feedline network, and (b) scattering parameters of feedline network.

4 | MEASURED RESULTS

The 1 × 4 feedline network to excite the 2 × 2 antenna array is shown in Figure 6a. The measured return-loss coefficients are done by Agilent vector network analyser 8722ES. Its S-parameter response in Figure 6b shows the feedline operates from 3.3 to 8.7 GHz for $|S_{11}| < -10$ dB. The antenna array was fabricated on FR4-substrate and has dimensions of the antenna array is 90 × 110 × 0.8 mm^3. The measured impedance bandwidths and AR of the proposed 2 × 2 CP slot-element array is shown in Figure 7. The antenna array operates across 3.2–9.0 GHz and has a fractional bandwidth of 94%. The array covers communications bands of WiMAX IEEE 802.16, C-band & ITUR-8 GHz. The array has an AR bandwidth of 4.3 GHz from 3 to 7.3 GHz which is wider than AR bandwidth reported in refs. [2–8]. The gain was measured using the

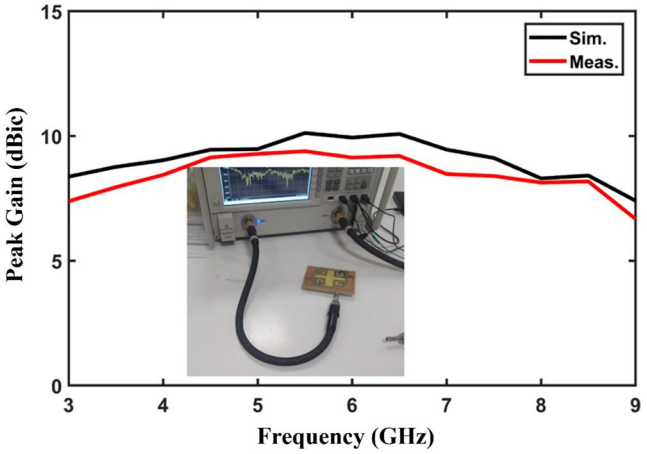

FIGURE 8 The gain of the proposed antenna.

FIGURE 7 (a) Simulated and measured return-loss of the final antenna array, and (b) axial-ratio response.

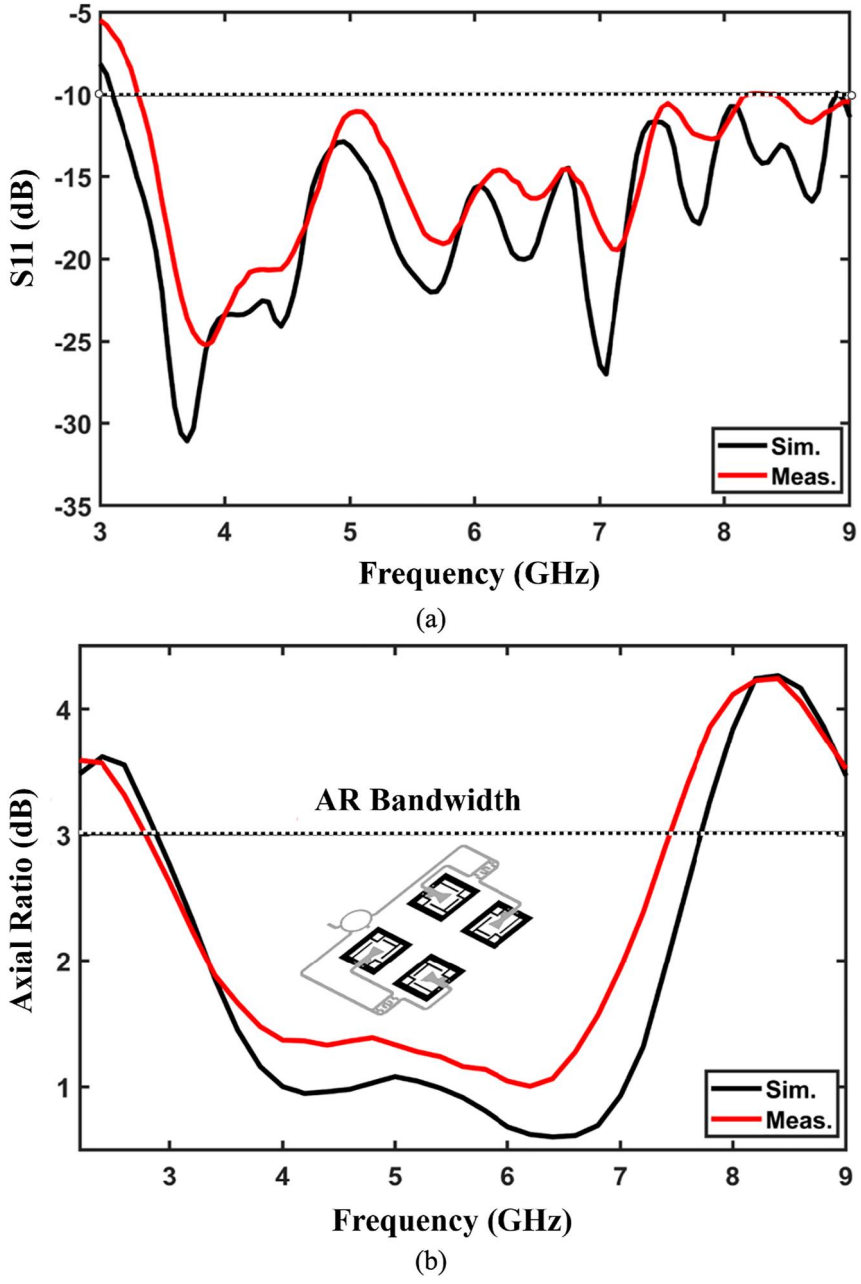

comparison method where the power of reference horn antenna and antenna under test were calculated separately. Then, by considering the relative difference and knowing the gain of standard horn antenna the gain of proposed antenna array was determined. Figure 8 shows the measured gain of the antenna array to be above 7.4 dBic and the peak gain is 11.5 dBic at 5.5 and 6.5 GHz. The normalised left-hand CP and right-hand circular polarisation (RHCP) radiation patterns of the array at $\varphi = 0^{o}$ for spot frequencies of 3.5 GHz, 5.5 and 7 GHz are shown in Figure 9. Across the frequency range between 3.5 and 7 GHz the array radiates essentially directionally. Also, due to the nature of feedline network, the antennas in the array are excited in a clockwise sequence resulting in a slightly larger RHCP pattern. There is good agreement between the simulation and measurement results. The discrepancies in the results are attributed to the non-ideal models used in the simulation, fabrication tolerances and unaccounted dispersion loss in the dielectric substrate. Salient parameters of the array are compared in Table 1. Compared to other cited works the proposed antenna offers significant improvement in impedance bandwidths, AR and fractional bandwidth with a high peak gain.

5 | CONCLUSION

A novel 2 × 2 CP antenna array configuration is shown to exhibit significantly improved impedance bandwidth for matching for $|S_{11}| < -10$ dB and enhanced AR. The array uses a couple of unique miniature double-box branch-line couplers and 180-degree rat-race. Miniaturisation is of the

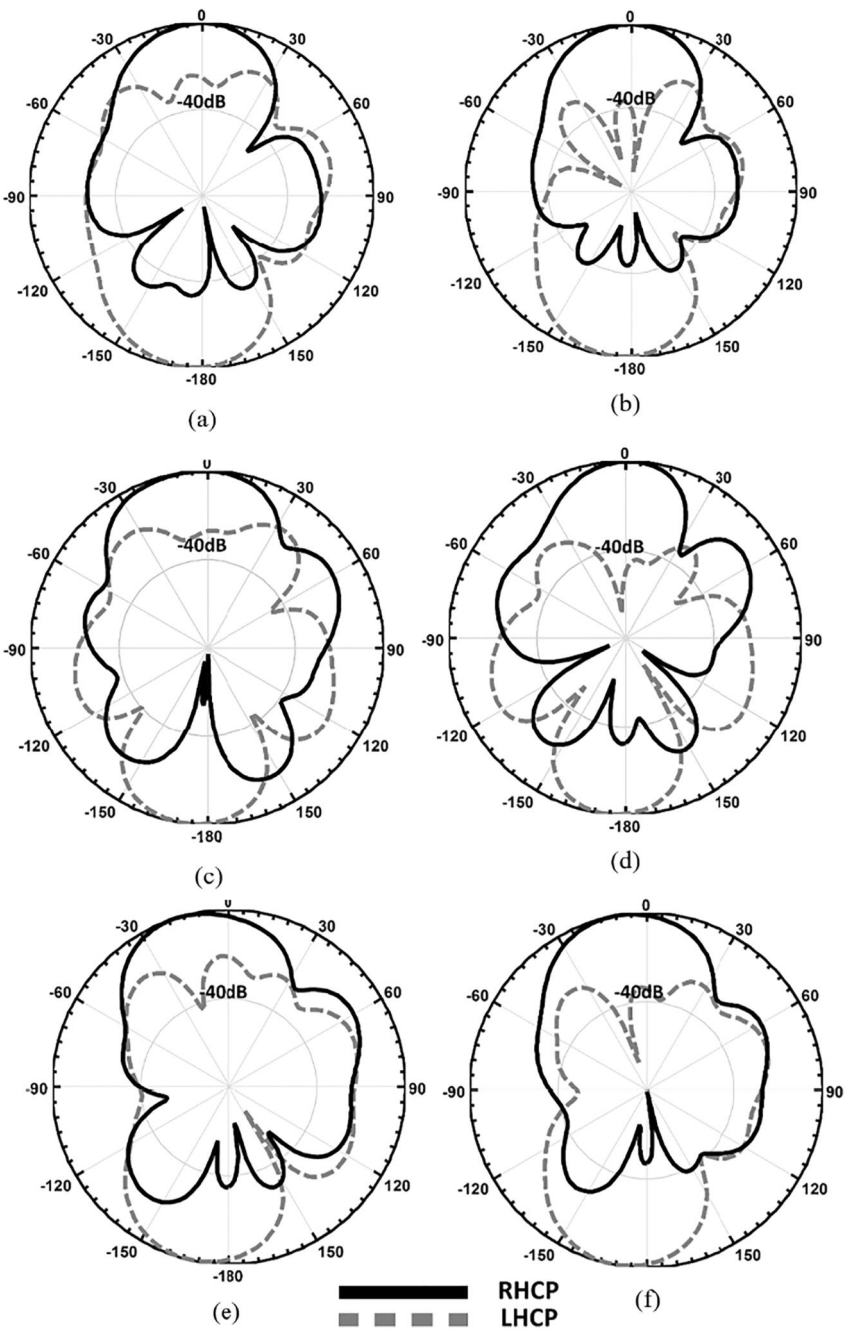

FIGURE 9 Measured RHCP & LHCP patterns at $\varphi = 0$, (a) measurement @ 3.5 GHz, (b) simulated @ 3.5 GHz, (c) measurement @ 5.5 GHz, (d) simulated @ 5.5 GHz, (e) measurement @ 7 GHz, and (f) simulated @ 7 GHz. LHCP, left-hand circular polarisation; RHCP, right-hand circular polarisation.

TABLE 1 Comparison of the proposed CP array with previous works.

Ref.	No. of layers	Structure complexity	Bandwidth (GHz)/ fractional bandwidth	CP bandwidth (GHz)/ fractional bandwidth	Dimensions ($\lambda_o \times \lambda_o \times \lambda_o$)	Peak gain (dBic)
[2]	Three	High	(4.2–7.5)/ 56.4%	(5–6.6)/27.5%	2.32 × 2.32 × 0.96	13
[3]	One	Low	(4–8.1)/68%	(4.9–6.45)/27%	1.7 × 1.7 × 0.015	8
[4]	Two	Medium	(9.7–12.3)/ 23.6%	(10.3–11.4)/ 10.1%	0.25 × 0.25 × 0.18	11.1
[7]	One	Low	(1.77–2.26)/ 24.3%	(1.78–1.8)/1.1%	0.29 × 0.29 × 0.06	1.72/2.17
			(3.84–5.38)/ 33.4%	(4.25–4.6)/7.9%		
[8]	Four	Very high	(2.01–2.3)/ 13.4%	(2.1–2.4)/13.3%	0.95 × 0.95 × 0.075	13
[15]	One	Low	(2.42–2.44)/ 40%	(2.39–2.49)/4%	0.76 × 0.76 × 0.013	10.4
[16]	One	Low	(1.92–4.25)/ 75%	(2.1–3.4)/47%	0.34 × 0.46 × 0.015	3.75
[17]	One	Low	-	(3.0–3.84)/24%	0.68 × 0.68 × 0.01	4
				(4.3–5.15)/18%		3
Proposed work	One	Low	(3.25–9)/93.8%	(3–7.3)/80%	1.54 × 1.88 × 0.014	11.5

Abbreviation: CP, circular polarisation.

coupler and it is achieved by loading the inside arms of the coupler with open-circuit stub to create a slow wave structure. The square-shaped ground loop encompassing the radiator is connected to the ground plane through metallic via holes, and the radiator is excited through CPW feedline. The measurements confirm the broadband performance of the array that covers communication bands of WiMAX IEEE 802.16, C-band, and ITU-R F386.9 systems. The antenna's measured impedance bandwidth of 5.75 GHz extends from 3.25 to 9 GHz for VSWR ≤2 and its 3 dB AR extends from 3 to 7.3 GHz. The average gain of antenna is 9.5 dBic.

AUTHOR CONTRIBUTIONS

Bal S. Virdee: Conceptualisation; validation; writing. **Tohid Aribi**: Conceptualisation; methodology; supervision; writing. **Tohid Sedghi**: Conceptualisation; methodology; writing.

ACKNOWLEDGEMENTS

This research is the consequence of a project agreed with the research committee at Urmia Branch, Islamic Azad University. Authors would like to appreciate, Urmia branch, Islamic Azad University, Urmia, Iran for its support. The author would like to appreciate Microwave & Antenna Research Center of Islamic Azad University Urmia Branch and London Metropolitan University for measuring the device.

CONFLICT OF INTEREST STATEMENT

The authors declare that there is no conflict of interest that could be perceived as prejudicing the impartiality of the research reported.

DATA AVAILABILITY STATEMENT

All the data in this manuscript is provided in this publication.

ORCID

Bal S. Virdee https://orcid.org/0000-0001-7203-0039
Tohid Sedghi https://orcid.org/0000-0003-3330-4804

REFERENCES

1. Sedghi, T., et al.: Small monopole antenna for IEEE 802.11a and X-bands applications using modified CBP structure. Wireless Pers. Commun. 80(2), 859–865 (2015). https://doi.org/10.1007/s11277-014-2045-z
2. Sharifi, G., et al.: Circularly polarized beam steering array antenna fed by low magnitude and phase error response of Butler matrix to use pattern stabilization applications. Int. J. RF Microw. Computer-Aided Eng. 32(3), 1–8 (2022). https://doi.org/10.1002/mmce.23022
3. Sedghichongaralouye-Yekan, T., Naser-Moghadasi, M., Sadeghzadeh, R. A.: Broadband circularly polarized 2×2 antenna array with sequentially rotated feed network for C-band application. Wireless Pers. Commun. 91(2), 653–660 (2016). https://doi.org/10.1007/s11277-016-3485-4
4. Monika, M., Rajput, A., Mukherjee, B.: Wideband circularly polarized low profile dielectric resonator antenna with meta superstrate for high gain. AEU-Int. J. Electron. Commun. 128, 1524–1535 (2021)
5. Sharifi, G., et al.: A high gain pattern stabilized array antenna fed by modified Butler matrix for 5G applications. AEU-Int. J. Electron. Commun. 122, 153237 (2020). https://doi.org/10.1016/j.aeue.2020.153237
6. Rafiei, V., et al.: Beam-steering high-gain array antenna with FP Bow-tie slot antenna element for pattern stabilisation. IET Microw., Antennas Propag. 14(11), 1185–1189 (2020). https://doi.org/10.1049/iet-map.2019.1071
7. Sung, Y.: Novel dual-band circularly polarized slot antenna with asymmetrical stubs. Microw. Opt. Technol. Lett. 62(12), 3966–3974 (2020). https://doi.org/10.1002/mop.32538
8. Dehnavi, M.S., Razavi, S.M.J., Armaki, S.H.M.: Improvement of the gain and the axial ratio of a circular polarization microstrip antenna by using a

metamaterial superstrate. Microw. Opt. Technol. Lett. 61(10), 2261–2267 (2019). https://doi.org/10.1002/mop.31886
9. Naser-Moghadasi, M., Ali-Sadeghzadeh, R., Sadeghzadeh, R.A.: A broad band circularly polarized cross slot cavity back array antenna with sequentially rotated feed network for improving gain in X-band application. Int. J. Microw. Wireless Tech. 9(3), 705–710 (2017). https://doi.org/10.1017/s1759078716000532
10. Kumar, A., Raghavan, S.: Broadband dual-circularly polarised SIW cavity antenna using a stacked structure. IIET Electron. Lett. 53(17), 1171–1172 (2017). https://doi.org/10.1049/el.2017.2407
11. Aribi, T., Naser-Moghadasi, M., Sadeghzadeh, R.: Circularly polarized beam-steering antenna array with enhanced characteristics using UCEBG structure. Int. J. Microw. Wireless Tech. 8(6), 955–962 (2016). https://doi.org/10.1017/s1759078715000318
12. Akhavan, H.G., Mirshekar-Syahkal, D.: Approximate model for microstrip fed slot antennas. Electron. Lett. 30(23), 1902–1903 (1994). https://doi.org/10.1049/el:19941300
13. Zheng, B., Sh, Z.: Effect of a finite ground plane on microstrip-fed cavity-backed slot antenna. IEEE Trans. Antenn. Propag. 53(2), 862–865 (2005). https://doi.org/10.1109/tap.2004.841278
14. Collin, R.E.: Foundation for Microwave Engineering, Ser. IEEE Electromagn. Wave Theory. IEEE Press, New York (1998). ch. 8
15. Lakshmi, M.L.S., Khan, H., Habibulla, B.T.P.: Novel sequential rotated 2×2 array notched circular patch antenna. J. Eng. Sci. Technol. Rev. 8(4), p73–77 (2015). https://doi.org/10.25103/jestr.084.11
16. Nasimuddin, X.Q., Chen, Z.N.: Dual-square-ring-shaped slot antenna for wideband circularly polarized radiation. Microw. Opt. Technol. Lett. 56(11), 2645–2649 (2014). https://doi.org/10.1002/mop.28663
17. Nasimuddin, Alphones, A., Jeevanandham, N.: Circularly polarized slot antennas with wideband performance. In: Asia-Pacific Microwave Conference (APMC), pp. 1–3 (2015)

How to cite this article: Virdee, B.S., Aribi, T., Sedghi, T.: Novel antenna array configuration using miniature double box branch-line couplers for wideband circularly polarised applications. IET Microw. Antennas Propag. 1–10 (2023). https://doi.org/10.1049/mia2.12388